Received: 4 May 2019 | Revised: 9 October 2019 | Accepted: 14 October 2019

DOI: 10.1111/jpi.12618

ORIGINAL ARTICLE

Journal of Pineal Research
Molecular, Biological, Physiological and Clinical Aspects of Melatonin

WILEY

Identification of a novel melatonin-binding nuclear receptor: Vitamin D receptor

Nan Fang[1] | **Chunyi Hu**[2] | **Wenqi Sun**[2] | **Ying Xu**[2] | **Yeqi Gu**[1] | **Le Wu**[1] | **Qing Peng**[1] | **Russel J. Reiter**[3] | **Lifeng Liu**[1]

[1]Department of Trauma Orthopaedics, Shanghai East Hospital, Tongji University School of Medicine, Shanghai, China

[2]State Key Laboratory of Molecular Biology, Institute of Biochemistry and Cell Biology, Shanghai Institutes for Biological Sciences, Chinese Academy of Sciences, Shanghai, China

[3]Department of Cellular & Structural Biology, UT Health Science Center, San Antonio, TX, USA

Correspondence
Lifeng Liu, Department of Trauma Orthopaedics, Shanghai East Hospital, Tongji University School of Medicine, Shanghai, China, 150 Jimo Road, Shanghai 200120, China.
Email: liulifengxy@163.com

Funding information
National Natural Science Foundation of China, Grant/Award Number: 81770870

Abstract

Previous studies confirmed that melatonin regulates Runx2 expression but the mechanism is unclear. There is a direct interaction between Runx2 and the vitamin D receptor (VDR). Herein, we observed a direct interaction between melatonin and the VDR but not Runx2 using isothermal titration calorimetry. Furthermore, this direct binding was detected only in the C-terminal ligand binding domain (LBD) of the VDR but not in the N-terminal DNA-binding domain (DBD) or the hinge region. Spectrophotometry indicated that melatonin and vitamin D3 (VD3) had similar uptake rates, but melatonin's uptake was significantly inhibited by VD3 until the concentration of melatonin was obviously higher than that of VD3 in a preosteoblastic cell line MC3T3-E1. GST pull-down and yeast two-hybrid assay showed that the interactive smallest fragments were on the 319-379 position of Runx2 and the N-terminus 110-amino acid DBD of the VDR. Electrophoretic mobility shift assay (EMSA) demonstrated that Runx2 facilitated the affinity between the VDR and its specific DNA substrate, which was further documented by a fluorescent EMSA assay where Cy3 labeled Runx2 co-localized with the VDR-DNA complex. Another fluorescent EMSA assay confirmed that the binding of the VDR to Runx2 was significantly enhanced with an increasing concentrations of the VDR, especially in the presence of melatonin; it was further documented using a co-immunoprecipitation assay that this direct interaction was markedly enhanced by melatonin treatment in the MC3T3-E1 cells. Thus, the VDR is a novel melatonin-binding nuclear receptor, and melatonin indirectly regulates Runx2 when it directly binds to the LBD and the DBD of the VDR, respectively.

KEYWORDS

interaction, melatonin, Runx2, vitamin D receptor, vitamin D3

1 | INTRODUCTION

Melatonin, an endogenously produced indoleamine discovered by Lerner and colleagues in 1958, is released by the vertebrate pineal gland during the daily period of darkness. It has multiple functions on many physiological processes, including modulation of circadian cycles, anti-osteoporosis, anti-aging, anti-antioxidant, anti-cancer, and anti-inflammatory.[1-4] As currently known, the regulation of the multiple functions of melatonin in cells is mediated by binding to its receptors in the plasma membrane or on the mitochondria membrane; these receptors include melatonin receptor types

1 (MT1 and MT2). Additionally, melatonin's antioxidant effects including its actions via MT3 (quinone reductase 2, NQO2) and its direct free radical scavenging actions have been described.[3]

Runt-related transcription factor 2 (Runx2), a member of Runx family, is a DNA-binding transcription factor which is essential for osteoblast development from mesenchymal stem cells (MSCs) and maturation into osteocytes; it also organizes crucial events during bone formation.[5] In mutant Runx2 mice, maturational arrest of osteoblasts blocks intramembranous and endochondral ossification completely.[6] The expression of Runx2 is essential for osteoblast differentiation, chondrocyte maturation and bone formation.[7-9] Moreover, Runx2 gene expression is associated with age-related changes in bone mineral density in the healthy young adult individuals.[10] Also, Runx2 highly correlates with osteoporosis where it coordinates a number of cellular events to directly regulate bone formation and bone resorption.[11,12] Thus, Runx2 has a positive action on bone, and up-regulation of its expression by melatonin contributes to osteoblast differentiation and reduces osteoporosis. Although MT2 plays a specific role in osteoblast differentiation from human MSCs,[13] Gao et al[14] reported that this effect of melatonin on Runx2 is not associated with MT1 and MT2 during chondrogenic differentiation of human MSCs. Furthermore, the precise regulatory mechanisms of melatonin are unclear.

Vitamin D receptor (VDR), a member of the nuclear receptor family,[15] is a transcription factor that plays important roles in calcium mobilization and bone formation.[5] The VDR can specifically bind the promoter regions of certain critical genes related to osteoblast differentiation and maturation to regulate the transcription and expression of these genes.[16] It is widely known that there is a functional relationship between Runx2 and the VDR.[17,18] For instance, Runx2 accounts for 70% in the VDR-binding site.[19] There is a functional cooperation between Runx2 and the VDR in the regulation of osteopontin transcription[20] and Runx2-mediated activation is further enhanced by cotransfection with the VDR.[21] Silencing the VDR or Runx2 attenuates the procalcific effects of vitamin D3 (VD3), and vascular calcification induced by high-dose VD3 is completely inhibited in the VDR knockout or Runx2 carboxy-terminus truncated heterozygous mice.[22] Stephens and Morrison[16] reported that Runx2 and the VDR combine to cooperatively regulate the expression of numerous genes. Moreover, the VDR may increase the expression levels of Runx2 by positively regulating calcium levels in primary renal tubular epithelial cells.[23]

Runx2 also interacts with the VDR in the promoter region of target genes, which can trigger a synergic activation of their transcription. This interaction involves a domain located in the C-terminal of the runt homology DNA-binding region of Runx2 and the N-terminal end of the VDR.[17,18] Furthermore, Runx2 at 209-361 position is sufficient to interact with the VDR.[24] Runx2 co-immunoprecipitates with the VDR protein present in nuclear extracts of rat osteoblasts, and their regulatory interaction is incorporated in the genetic program involved in the specification and differentiation of osteoblasts.[25] Recently, Prado et al[26] demonstrated that melatonin also has a positive effect on the regulation of the VDR although its regulation is primarily by binding VD3 to regulate serum calcium levels which indirectly influences bone formation and osteoblast differentiation. However, the interactive relationship between melatonin and the VDR has not been examined although they play essential roles in bone formation and bone resorption.

Herein, we demonstrate that melatonin indirectly regulates Runx2 when it directly binds to the ligand binding domain (LBD) and the DNA-binding domain (DBD) of the VDR, respectively; this suggests that the VDR is a novel melatonin-binding receptor. Interestingly, melatonin and VD3 have similar uptake rates, but melatonin's uptake is significantly inhibited by VD3 until the concentration of melatonin is obviously higher than that of VD3 in a preosteoblastic cell line MC3T3-E1. Runx2 facilitates the affinity between the VDR and its specific DNA substrate. Furthermore, this direct interaction between the VDR and Runx2 is markedly enhanced by melatonin treatment. Information garnered from this study could be helpful for further exploring the mechanism of melatonin how to promote osteoblast differentiation and for identifying more melatonin receptors through homologous structure of the VDR's hormone receptor binding domain and the similar regulatory mechanisms.

2 | MATERIAL AND METHODS

2.1 | Protein expression and purification

The Runxs and VDR clone cDNA fragments were obtained from human embryonic kidney (HEK 293) cells. *Homo sapiens* Runxs and VDR full length and fragment genes were cloned into a modified pET28b vector with a SUMO protein fused at the N-terminus after the 6xHis tag. The proteins were expressed in *Escherichia coli* BL21 (DE3). After induction for 16 hours with 0.2 mmol/L IPTG at 16°C, the cells were harvested and resuspended in lysis buffer (50 mmol/L Tris-HCl pH 8.0, 500 mmol/L NaCl, 10% glycerol, 1 mmol/L PMSF, 2 mmol/L 2-mercaptoethanol, and a home-made protease inhibitor cocktail). The 100 × home-made protease inhibitor cocktail included 100 mmol/L PMSF, 100 mg/mL benzamidine, 100 g/mL leupeptin, 100 g/mL aprotinin and 100 g/mL pepstatin. After sonication and centrifugation, the supernatant was mixed with Ni-NTA agarose beads (Qiagen) and rotated for 1 hours at 4°C. Then, Ulp1 protease was added at a molar ratio of 1:200 to remove the 6xHis and SUMO tag at the N-terminus of the VDR proteins. The VDR proteins were collected after on-beads Ulp1 digestion for 12 hours at

4°C and were further purified by gel-filtration chromatography on Hiload Superdex200 column (GE Healthcare) equilibrated with buffer (25 mmol/L Tris-HCl pH 8.0, 150 mmol/L NaCl). The purified proteins were concentrated to 10 mg/mL and stored at − 80°C. The GST-tagged VDR was cloned and purified from pGEX-6p-1 vector. After induction for 16 hours with 0.2 mmol/L IPTG at 16°C, the cells were harvested and resuspended in lysis buffer (50 mmol/L Tris-HCl pH 8.0, 400 mmol/L NaCl, 10% glycerol, 1 mmol/L PMSF, 5 mmol/L DTT and the home-made protease inhibitor cocktail). After sonication and centrifugation, the supernatant was mixed with glutathione-sepharose 4B (GE) and rotated for 2 hours at 4°C. After elution by 15 mmol/L GSH, the eluted proteins were further purified by gel-filtration chromatography on Hiload Superdex200 column (GE Healthcare) equilibrated with buffer (25 mmol/L Tris-HCl pH 8.0, 150 mmol/L NaCl). The fractions containing the proteins were collected and analyzed.

2.2 | Isothermal titration calorimetry (ITC)

The equilibrium dissociation constants of interactions were determined by using an ITC 200 calorimeter (MicroCal). Firstly, we dissolved melatonin (Sigma) in dimethyl sulfoxide (DMSO) solution at 50 mmol/L concentrations. Then, melatonin solution was diluted to 1 mmol/L using the ITC buffer (25 mmol/L Tris pH8.0, 150 mmol/L NaCl). 0.5 mmol/L purified VDR protein stock was diluted to 0.1 mmol/L using the ITC buffer. Then, melatonin and VDR protein sample were put in 1000 mL ITC buffer to dialysis for 6 hours using 3.5 kDa dialysis membrane cut off. Following dialysis, we used the melatonin to titrate the VDR. Every 90 seconds, 2 μL melatonin solution at 1 mmol/L concentrations would be injected into 0.1 mmol/L VDR solution. The enthalpies of binding between melatonin (1000-1500 μmol/L) and Runx2 (100-150 μmol/L) or the VDR (100-150 μmol/L) were measured at 20°C in 20 mmol/L Tris-HCl (pH 8.0) and 150 mmol/L NaCl. Two independent experiments were performed for every interaction described herein. The ITC data were subsequently analyzed and fitted with one binding site model using Origin 7 software (OriginLab) with blank injections of melatonin into buffer subtracted from the experimental titrations prior to data analysis.

2.3 | Cell culture and melatonin preparation

Mouse preosteoblastic cell line MC3T3-E1 cells were cultured in a Minimum Essential Medium α (Gibco; Thermo Fisher Scientific), supplemented with 10% fetal bovine serum (FBS) (HyClone; Thermo Fisher Scientific), in a humidified 5% CO_2 atmosphere at 37°C with the medium being changed every other day. The cells were utilized in passages 7-11. Melatonin solution was prepared as follows: starting from a melatonin stock solution in 100% DMSO and serial dilutions with culture media in accordance with the tested doses were done. This ensured that culture media contain 0.2% DMSO at every concentration of melatonin or vehicle group.

2.4 | Spectrophotometry

VD3 and 1,25-$(OH)_2$-vitamin D3 (1,25$(OH)_2$VD3) were obtained from Sigma. The MC3T3-E1 cells were seeded in 6-well plates at a density of 4×10^5 cells per well under regular culturing conditions. After culturing 6 days, they were washed three times with PBS. Then, 1.5 mL samples diluted with PBS were added to each well. The cells were randomly divided into five groups: VD3 (VD3 at 5 μg/mL concentrations), melatonin (melatonin at 5 μg/mL concentrations), melatonin + VD3 (5 μg/mL) (melatonin at 5 μg/mL concentrations plus VD3 at 5 μg/mL concentrations), melatonin + VD3 (0.2 μg/mL) (melatonin at 5 μg/mL concentrations plus VD3 at 0.2 μg/mL concentrations), and melatonin + 1,25$(OH)_2$VD3 (0.2 μg/mL) (melatonin at 5 μg/mL concentrations plus 1,25$(OH)_2$VD3 at 0.2 μg/mL concentrations). After 4 hours incubation, 0.75 mL of the supernatant was taken out from each well and then centrifuged at 6000 *g* for 5 minutes. The concentration of VD3 or melatonin was determined by ultraviolet spectrophotometer under 352 nm or fluorescence spectrophotometer under Ex 227.96 nm and Em 352 nm, respectively.

2.5 | GST pull-down assays

GST-tagged VDR with different Runx2 fragments, and 10 μL glutathione-sepharose 4B beads were suspended with 50 μL of binding buffer (25 mmol/L Tris, pH 8.0 and 100 mmol/L NaCl, 10% glycerol). 30 μg GST-tagged VDR and 30 μg purified Runx2 proteins were added into the suspension beads and incubated at 4°C for 40 minutes. The beads were washed three times with 150 μL binding buffer. The bead-bound proteins were eluted by 50 μL SDS-PAGE sample loading buffer. The protein samples were analyzed with SDS-PAGE, followed by immunoblotting and coomassie brilliant blue (CBB) gel staining.

2.6 | Yeast two-hybrid (Y-2-H)

Yeast cell growth and manipulation were done according to standard procedures.[27] The yeast strain L40 (MATa his3Δ200 trp1-901 leu2-3112 ade2 LYS::(4lexAop-HIS3) URA3::(8lexAop-LacZ)GAL4) was used in this study. The yeast two-hybrid assays were performed with two plasmids: pBTM116 (binding domain) and pACT2 (activation domain). The colonies containing both plasmids were selected

on -Leu -Trp plates. Then, we used histidine and adenine absent media (-His, -Ade) to screen the interaction.

2.7 | Electrophoretic mobility shift assay (EMSA)

The sequence of the DNA template used for the assay was 5′-ATCTTAATTATATTATATAGG-3′. Proteins of the VDR at 0-320 nmol/L concentrations or the VDR plus Runx2 at 10 μmol/L concentrations in binding buffer (25 mmol/L Tris-HCl, pH 8.0, 100 mmol/L NaCl, 2 mmol/L DTT, and 10% glycerol) were mixed with 25 nmol/L FAM-labeled dsDNA probe in a total volume of 15 μL. The reaction mixtures were incubated at room temperature for 30 minutes before being loaded onto a 6% nondenaturing polyacrylamide gel. The gels were then dried and visualized on Bio-Rad PharosFX Plus.

2.8 | Cy3 fluorescence labeling of $Runx2_{310\text{-}390}$

We used Cy3 fluorescence to label Runx2 310-390 peptide (in principle, Cy3 labeling at cysteine amino acid). The fluorescence tracks Runx peptide trace in the native gel. We took 100 μL peptide at 200 μmol/L concentrations, then added 10 μL Cy3 dye at 20 mmol/L concentrations (at a 1:10 molar ratio). This was mixed and put on ice for 30 minutes, then loaded the reaction solution on a 5 mL de-salt column to remove the free dye, finally collected the first 600 μL sample from the column for research study.

2.9 | Co-immunoprecipitation (co-IP)

The MC3T3-E1 cells were plated at 10^4 cells/cm^2 for 24 hours before treatment. Thereafter, they were treated with melatonin dissolved in 0.2% DMSO or vehicle (0.2% DMSO in culture medium only) media containing 10% FBS. After treatment with or without melatonin for 24 hours, the MC3T3-E1 cell extracts were prepared by lysis buffer (10 mmol/L KCl, 1.5 mmol/L $MgCl_2$, 10 mmol/L HEPES, 150 mmol/L NaCl, 1% Triton X-100, 1 mmol/L DTT) supplemented with a complete protease inhibitor cocktail (Roche). After cells were broken by ultrasonic waves, the extracts were centrifuged at 12 000 g for 15 minutes at 4°C, and then, the supernatants containing total protein were harvested. Equal amounts of lysates were incubated with the Flag antibody for 3 hours at 4°C before adding protein A/G agarose (Santa Cruz Biotechnology) for another 2 hours. The immunoprecipitates were washed extensively three times with lysis buffer, boiled, and microcentrifuged. Then, the immunoprecipitates were subjected to immunoblot assays with monoclonal antibodies against Flag or Myc. To ensure the data validity and repeatability, the MC3T3-E1 cells used in the experiments were from the same treated batch.

2.10 | Statistical analysis

Data were analyzed using SPSS 16.0 software. An independent-samples t test or a one-factor analysis of variance was used to evaluate the differences between groups with various treatments, and least significant difference (LSD) test was

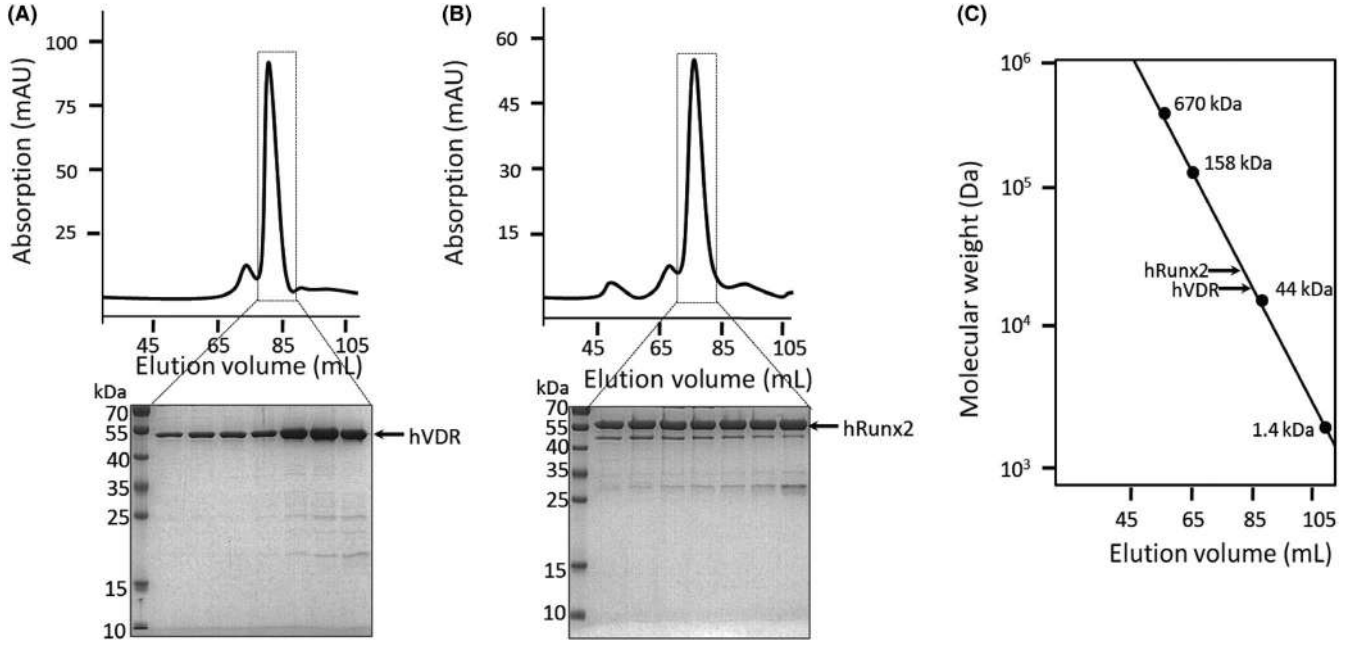

FIGURE 1 Purification and characterization of the VDR and Runx2 proteins. A, The gel filtration (Hiload Superdex200) and SAD-PAGE of the hVDR. B, The gel filtration (Hiload Superdex200) and SAD-PAGE of hRunx2. C, The molecular size calculation by standard sample in Hiload Superdex200. At least three independent experiments were performed. Representative results were present

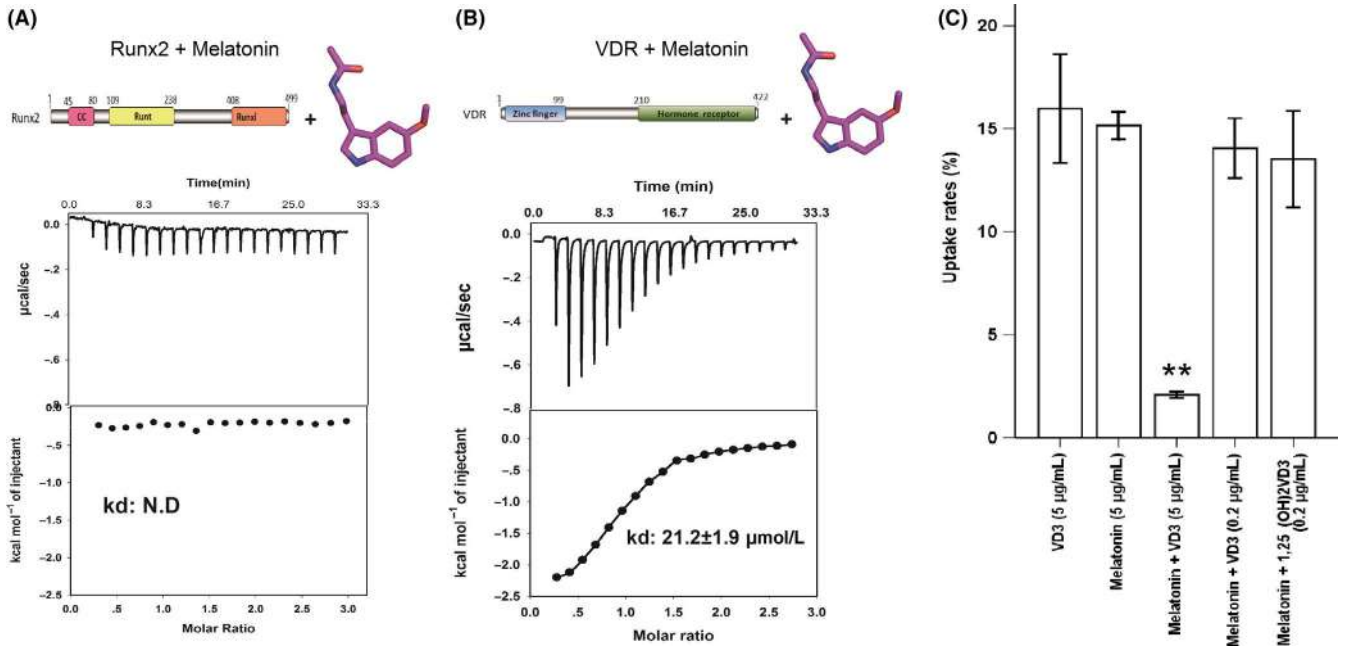

FIGURE 2 Test for the interaction between melatonin and Runx2 or the VDR and the competitive binding of the VDR by melatonin or the VDR's natural ligand. The ITC assay between melatonin and (A) Runx2 or (B) VDR was performed using 1 mmol/L melatonin titrating 0.1 mmol/L Runx2 or the VDR. C, The spectrophotometry assay for VD3 and melatonin was performed to evaluate their uptake rates in a preosteoblastic cell line MC3T3-E1. The cells were randomly divided into five groups: VD3 (VD3 at 5 µg/mL concentrations), melatonin (melatonin at 5 µg/mL concentrations), melatonin + VD3 (5 µg/mL) (melatonin at 5 µg/mL concentrations plus VD3 at 5 µg/mL concentrations), melatonin + VD3 (0.2 µg/mL) (melatonin at 5 µg/mL concentrations plus VD3 at 0.2 µg/mL concentrations), and melatonin + 1,25$(OH)_2$VD3 (0.2 µg/mL) (melatonin at 5 µg/mL concentrations plus 1,25$(OH)_2$VD3 at 0.2 µg/mL concentrations). The uptake rate of VD3 or melatonin was calculated in accordance with the percent of drop in their concentrations in the media, which was determined by ultraviolet spectrophotometer for VD3 under 352 nm or fluorescence spectrophotometer for melatonin under Ex 227.96 nm and Em 352 nm. $^{**}P < .01$, compared with VD3, melatonin, melatonin + VD3 (0.2 µg/mL), or melatonin + 1,25$(OH)_2$VD3 (0.2 µg/mL). Data were expressed as mean ± SEM. At least three independent experiments were performed. Representative results were present

used for post hoc subgroup analysis. All data were presented as mean ± SEM of at least three independent experiments. Results were considered statistically significant when the *P*-value was less than .05. Finally, representative figures were present.

3 | RESULTS

3.1 | Purification and characterization of the VDR and Runx2 proteins

To clarify the interaction between proteins, we purified the VDR and Runx2 proteins using *Escherichia coli* (BL21 DE3) expression system. After purification, we used size-exclusion to analyze the characterization of proteins. As shown in Figure 1, high quality (a) VDR and (b) Runx2 protein samples were obtained by systematically screening and optimizing for expressive vectors, expressive systems, expressive conditions and purification steps. The elution volume from size-exclusion profiles suggests that purified VDR and Runx2 proteins exist in solution as a monomer (c).

3.2 | There is a direct interaction between melatonin and the VDR but not Runx2, and melatonin and VD3 compete with each other to bind to the VDR

Because melatonin easily penetrates cytomembrane to enter into cells, we tested whether there is a direct interaction between melatonin and Runx2. We conducted an exploratory study by the ITC in which melatonin at 1 mmol/L concentrations was used to titrate the Runx2 protein at 0.1 mmol/L concentrations. As shown in Figure 2A, no exothermy or endothermy was found, which suggests that there is no direct interaction between them and melatonin does not directly regulate Runx2.

Taking into consideration that there is a direct interaction between Runx2 and the VDR expressed primarily in the cell nucleus, a transcription factor the same as Runx2 in osteoblast differentiation and maturation, we speculated whether melatonin may directly bind to the VDR to indirectly regulate Runx2. Thus, we examined the interaction between melatonin and the VDR using the ITC. The VDR protein at 0.1 mmol/L concentrations was titrated with melatonin at

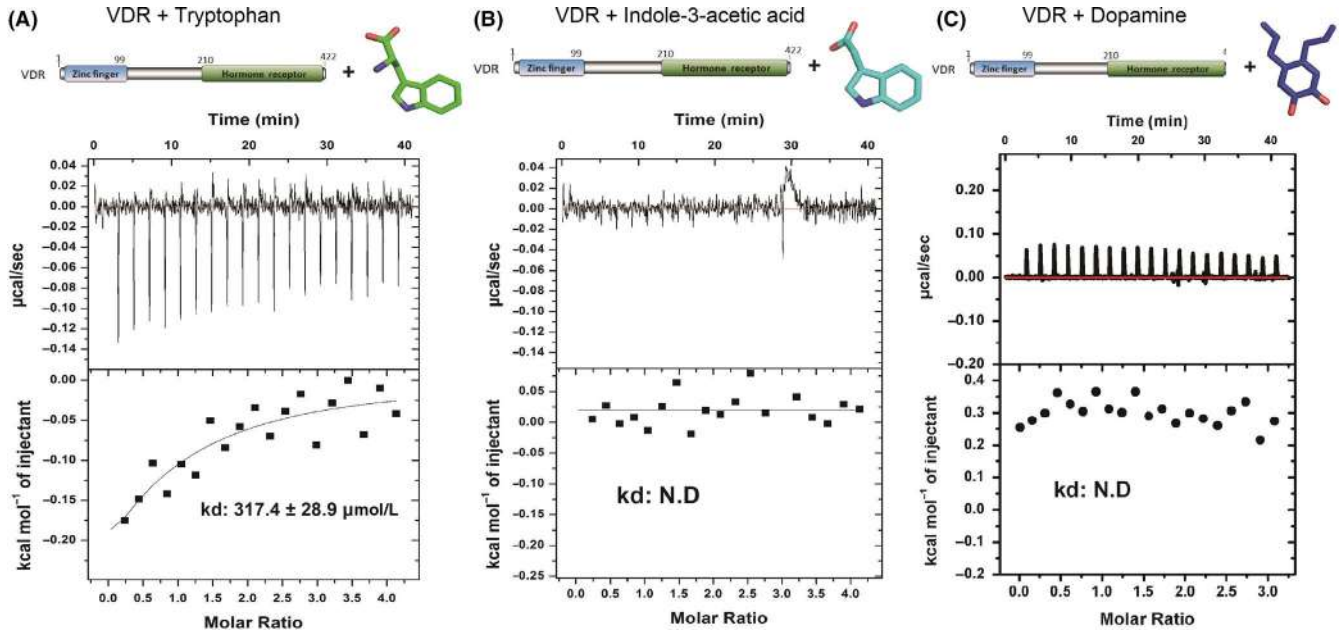

FIGURE 3 Test for the interaction between other small indole molecules and the VDR. The ITC assay between other small molecules (A, tryptophan; B, indole-3-acetic acid; C, dopamine) and the VDR was performed using 1 mmol/L these molecules titrating 0.1 mmol/L VDR. At least three independent experiments were performed. Representative results were present

1 mmol/L concentrations at 20°C. We found that melatonin was capable of binding with the VDR; the Kd values were 21.2 ± 1.9 µmol/L (Figure 2B).

Since $1,25(OH)_2VD3$ formed by VD3 is the natural ligand of the VDR[28] and VD3 and melatonin have similar binding affinities for the VDR,[29] we tested whether there is a competitive binding of the VDR by melatonin or VD3. To accomplish this, we examined their binding abilities to the VDR in the MC3T3-E1 cells using spectrophotometry. Melatonin and VD3 had similar uptake rates (~15%) when they were individually added to the MC3T3-E1 cells at 5 µg/mL concentrations. However, melatonin's uptake was significantly decreased to ~ 2% when VD3, at the same concentrations, was simultaneously added. Interestingly, melatonin's uptake rates were almost recovered to original levels when VD3 was added at 0.2 µg/mL concentrations even in the presence of $1,25(OH)_2VD3$ (0.2 µg/mL) with the highest activity (Figure 2C). Thus, the competitive binding ability of VD3 was significantly inhibited when the concentration of melatonin was obviously higher than that of VD3 or $1,25(OH)_2VD3$. These findings suggest that these molecules, to some extent, compete with each other to bind to the VDR.

3.3 | Other small indole molecules do not effectively bind to the VDR

Since melatonin is a small indole molecule, we selected other simple indole molecules based on their structural similarities, including tryptophan (Trp), indole-3-acetic acid (IAA) and dopamine, to further validate that there was a direct interaction between melatonin and the VDR. We tested the interaction between these small molecules and the VDR using the ITC. The VDR protein at 0.1 mmol/L concentrations was titrated with Trp, IAA or dopamine at 1 mmol/L concentrations at 20°C. We found that Trp maintained a little affinity for the VDR with 317.4 ± 28.9 µmol/L Kd (Figure 3A). However, both IAA and dopamine had no affinity for the VDR (Figure 3B,C). These results indicate that it is not that all small indole molecules have the ability to bind to the VDR.

3.4 | There is a direct binding between melatonin and the LBD of the VDR but not the DBD or the hinge region

To further identify how melatonin binds with the VDR, we analyzed the VDR structure. The VDR can be divided into the following domains: N-terminus, a zinc finger binding domain (also named the DBD), C-terminus, a hormone receptor binding domain (also named the LBD)[30] and a hinge region between them which enables flexibility for dimerization (Figure 4A).[31] The VDR is a member of steroid hormone receptor superfamily. The conventional steroid hormone is usually composed of a benzene ring and a phenyl hydroxy group, plus some carbon side chains, such as glucocorticoid. By analogy of structures of melatonin, epinephrine, and glucocorticoid, we noticed that they had structural similarities.

The VDR was, therefore, subdivided into several fragments (Figure 4B). We examined interactions between these fragments and melatonin. The results showed that only

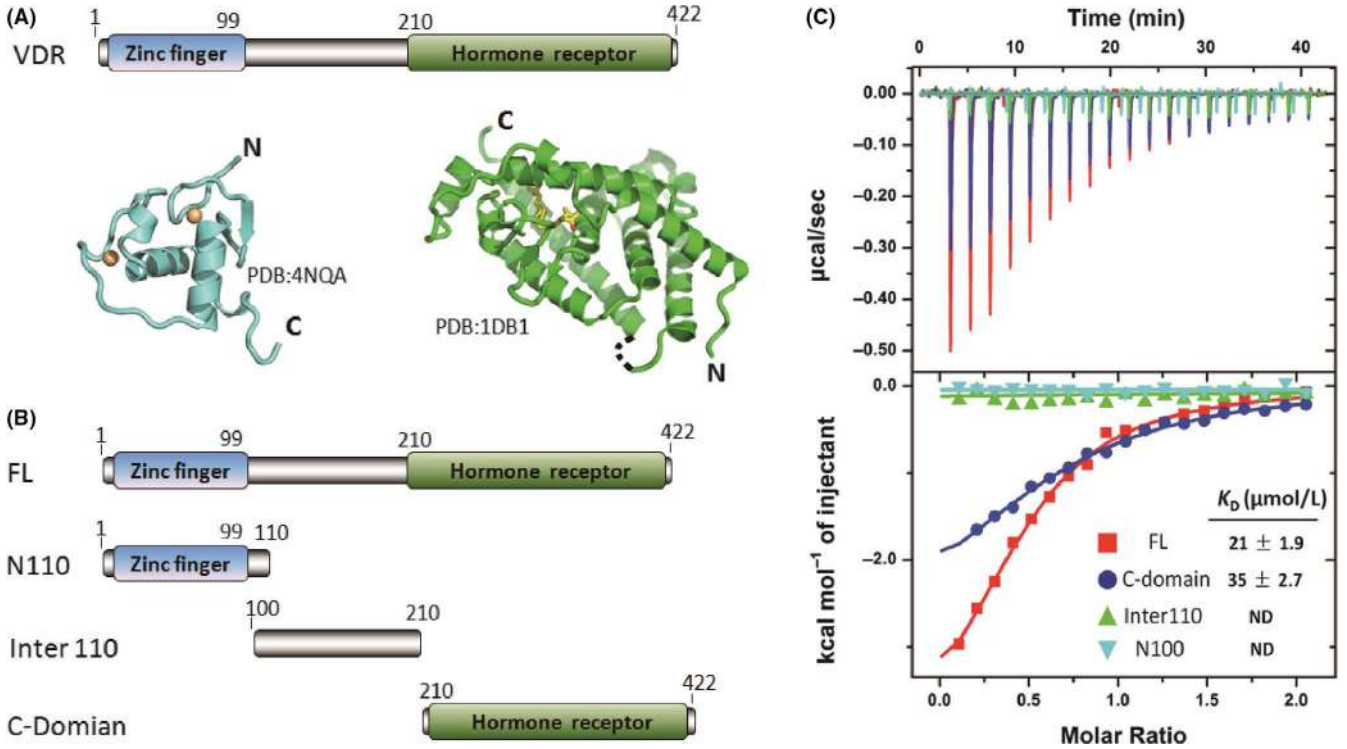

FIGURE 4 Structural and interaction domain analysis of the VDR-melatonin complex. A, The domain organization and overall structure of the VDR (the N-terminal zinc finger domain, PDB: 4NQA; the C-terminal hormone domain, PDB: 1DB1). B, The constructions of *Homo sapiens* VDR for the VDR-melatonin interaction analysis. C, The ITC assay was conducted for the different constructs using 1 mmol/L melatonin titrating 0.1 mmol/L VDR's full length (FL), C-domain, 100-210 (Inter110) and 1-100 (N100) of N-terminus. At least three independent experiments were performed. Representative results were present

C-terminal domain containing the LBD of the VDR directly bound to melatonin while no interaction was detected in other regions. The interactive Kd values were 35 ± 2.7 µmol/L (Figure 4C). Therefore, there was a direct binding between melatonin and the C-terminal LBD of the VDR but not the N-terminal DBD (N100) or the hinge region of the VDR (Inter110).

3.5 | The N-terminus 110-amino acid DBD of the VDR interacts with the 319-379 position of Runx2

Previous studies have reported that the N-terminal end of the VDR binds directly with the C-terminal DNA-binding region of Runx2[17,18] and Runx2 at 209-361 position is sufficient to interact with the VDR,[24] which makes it possible that the VDR links with the regulation of melatonin to Runx2. To further identify the smallest segment of interaction between the VDR and Runx2, we performed a GST pull-down assay. Firstly, we applied the purified GST-fused VDR_FL (VDR full length) and various Runx2 truncations to perform a GST pull-down experiment (Figure 5A). The results showed that the smallest fragment of Runx2 interacting with the VDR_FL was approximately on the 319-398 position (Figure 5B). Secondly, we performed a GST pull-down assay between the Runx2_300-379 region and the VDR_FL or the VDR truncations (Figure 5C). Based on the results from the comparison, we confirmed that the minimum region of Runx2 combined with the VDR was on the 319-379 position (about 60 amino acid regions) (Figure 5B). Similarly, we examined the smallest fragment of the VDR interacting with Runx2. The results suggested that the smallest region at which the VDR interacts with Runx2 was at the N-terminus 110-amino acid DBD of the VDR (Figure 5D).

Because we used GST-tagged VDR or Runx2, a control GST pull-down assay was performed using GST empty protein pulling down Runx2 or the VDR fragments to check whether there is a nonspecific interaction between GST tag and Runx2 or the VDR. The results showed that there was no nonspecific interaction between GST and Runx2 or the VDR (Figure 5E), which validates that the results of GST pull-down are reasonable and reliable. So far, our interactive analyses were based on in vitro assay. So, we did yeast two-hybrid (Y-2-H) assay to study the interaction to mimic in vivo conditions. We used Gal4's DNA-binding domain (BD, pBTM vector) fused Runx2's different fragments to bait the Gal4's activation domain (AD, pACT vector) fused VDR (Figure 5F). As we expected, the results of Y-2-H assay were consistent with the in vitro GST pull-down assay, which suggests that our interactive analysis also exists in vivo.

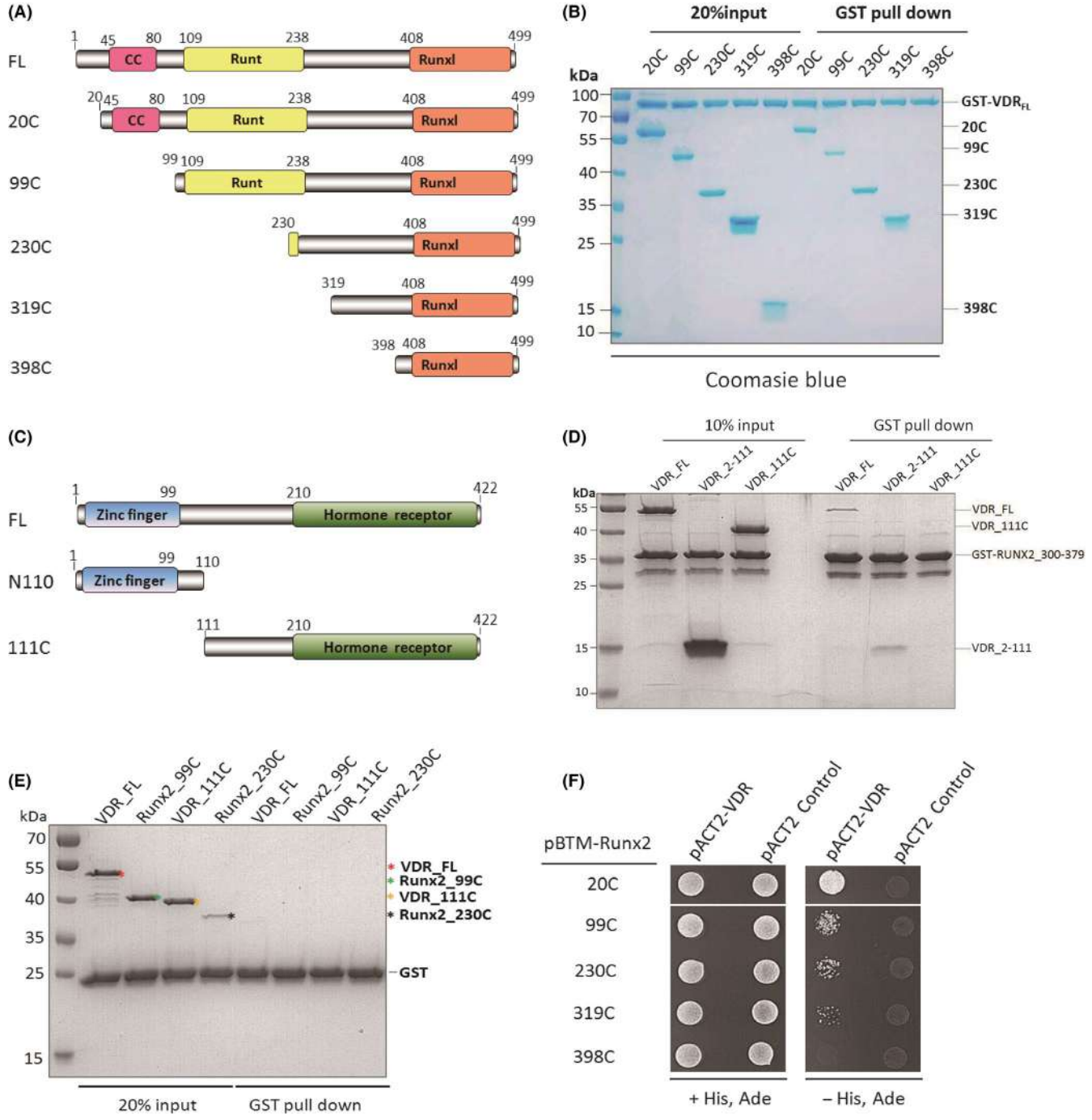

FIGURE 5 Interactive analyses between the VDR and Runx2. A, Summary of Runx2 constructs used for mapping the minimum VDR-binding motif of Runx2. B, GST pull-down assays identified the minimum Runx2 region responsible for binding to the VDR_{FL}. C, Summary of the VDR constructs used for mapping the Runx2-binding motif of the VDR. D, GST pull-down assays identified the VDR region responsible for binding to $Runx2_{300\text{-}379}$. E, The GST pull-down assay used GST empty protein to test the VDR and Runx2's nonspecific interaction with GST tag. F, Yeast two-hybrid assay to study the interaction between Runx2's fragments and the VDR in the mimic in vivo conditions

3.6 | Runx2 facilitates the affinity between the VDR and its specific DNA substrate, and melatonin enhances the direct interaction between the VDR and Runx2

Since the VDR is capable of binding DNA sequences, we tested whether Runx2 enhances the binding ability of the VDR with its specific DNA sequences. We found that the VDR was mainly biased toward AT DNA-binding sequence and designed its specific DNA-binding sequences in accordance with reports of Shaffer and Gewirth.[32] The designed DNA-binding sequence (FAM-DNA_{VDR}) was FAM-5′ATCTTAATTATATTATATAGG-3′. EMSA assay was performed at the N-terminus 110-amino acid DBD of the

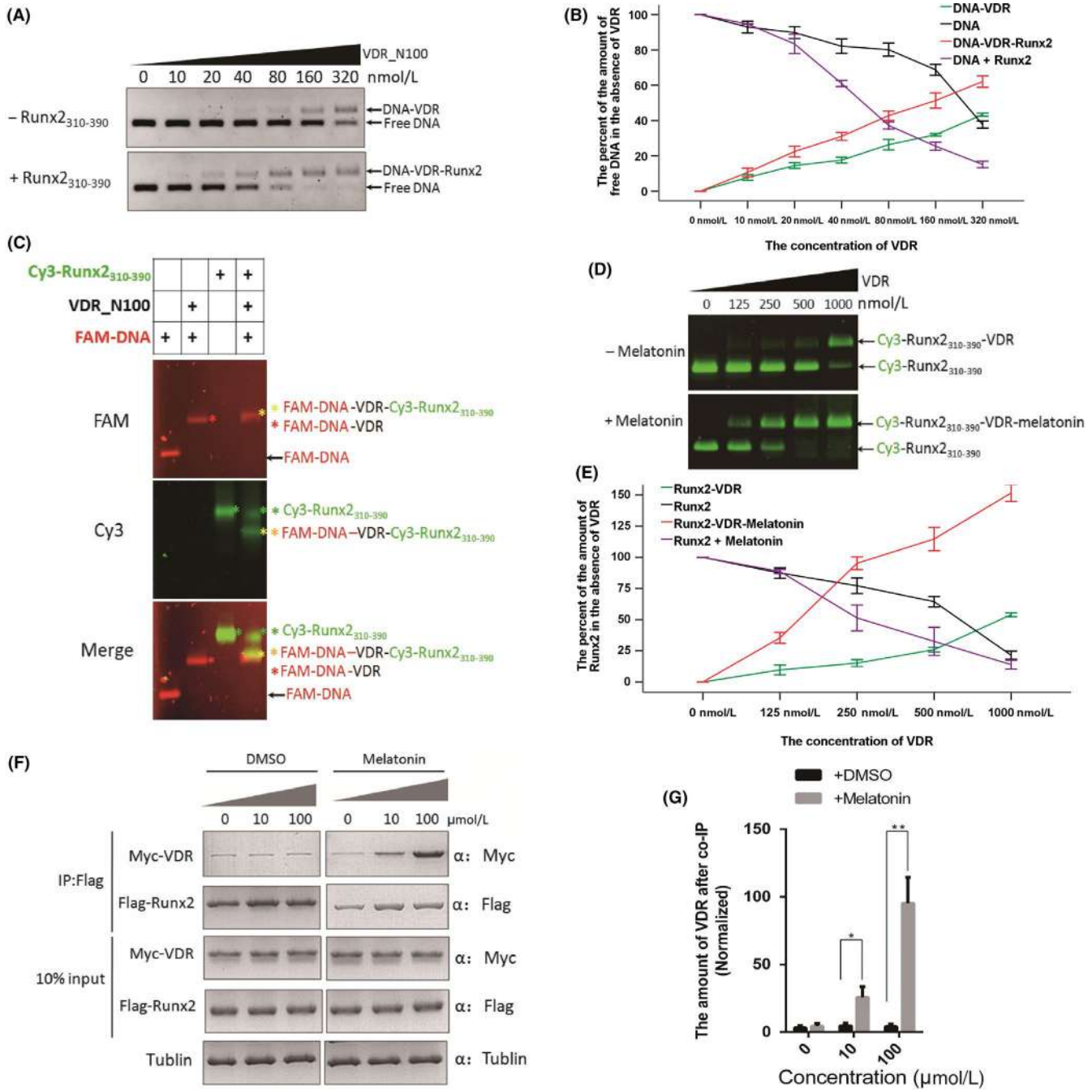

FIGURE 6 Characteristics of the interaction between the VDR and Runx2. A, EMSA assays of the VDR_{N100} with 25 nmol/L FAM-labeled dsDNA in the absence (−) or presence (+) of 10 μmol/L $Runx2_{310\text{-}390}$ (dsDNA: 5'-ATCTTAATTATATTATATAGG-3'). B, The quantified results based on the percent of the amount of free DNA in the absence of the VDR in the EMSA assay. C, The EMSA assay to identify the co-localization of $Runx2_{310\text{-}390}$ and DNA-VDR_{N100} complex. D, The EMSA assay to titrate the affinity values between Cy3 labeled Runx2 and the VDR in presence or absence of 10 μmol/L melatonin. E, The quantified results based on the percent of the amount of Cy3 labeled $Runx2_{310\text{-}390}$ in the absence of the VDR in the EMSA assay. F, Co-immunoprecipitation (co-IP) of the MC3T3-E1 cells expressing Myc-VDR and Flag-Runx2 in melatonin at 0, 10, or 100 μmol/L concentrations. Flag antibody was used for immunoprecipitation. G, The quantified results based on the amount of normalized proteins from co-IP. $^{*}P < .05$ or $^{**}P < .01$, compared with control group of DMSO. Data were expressed as mean ± SEM. At least three independent experiments were performed. Representative results were present

VDR (VDR_2-111). We found that the binding of the VDR with its specific DNA sequences was markedly enhanced with the increasing concentrations of the VDR, especially in the presence of 10 μmol/L $Runx2_{310\text{-}390}$ (Figure 6A,B).

Since a higher shift band (Runx2-VDR-DNA ternary complex) after adding Runx2 peptide has not been shown, this is not sufficient to conclude that Runx2 increases the VDR's DNA-binding activity by binding with the VDR. So, a

fluorescent EMSA assay was conducted to track whether Cy3 labeled Runx2 co-localizes with the VDR-DNA complex. In this assay, we clearly documented the DNA, the VDR-DNA complex and Cy3 labeled Runx2 bands (Figure 6C; lane 1, 2, and 3). Interestingly, when only Cy3-Runx2 peptide was loaded, we observed one green band on the gel. However, if Cy3-Runx2 with the VDR-DNA complex were loaded, we observed two bands of Cy3-Runx2 (Figure 6C; lane 4), which suggests that Cy3-Runx2 co-localizes with the VDR-DNA complex. Overall, Runx2 indeed promotes the VDR's DNA-binding activity by interacting with the VDR directly.

We then performed another fluorescent EMSA assay using Cy3 labeled Runx2 peptide with the VDR in the presence or absence of 10 μmol/L melatonin (Figure 6D). In this assay, the binding of the VDR to $Runx2_{310\text{-}390}$ was significantly enhanced with an increasing concentrations of the VDR, especially in the presence of 10 μmol/L melatonin (Figure 6E). This in vitro assay shows that melatonin can enhance the direct interaction between the VDR and Runx2.

To further verify whether melatonin enhances the direct interaction between the VDR and Runx2, we transfected preosteoblastic cell line MC3T3-E1 with Myc-VDR and Flag-Runx2 plasmids. The MC3T3-E1 cells were randomly divided into three groups and treated with 0.2% DMSO, melatonin (dissolution with 0.2% DMSO) at 10 μmol/L or 100 μmol/L concentrations for 12 hours. Then, we applied Flag antibody for co-IP assay. As shown in Figure 6F, there was a significantly progressive increase in the amount of Myc-VDR co-immunopecipitated with Flag antibody, compared with the control group, when exogenous melatonin was gradually increased. The findings suggest that melatonin markedly enhances the direct interaction between the VDR and Runx2 in the MC3T3-E1 cells. In accordance with the quantified results, we observed a significant effect of melatonin on promoting the binding of the VDR with Runx2 (Figure 6G).

4 | DISCUSSION

Melatonin is involved in many physiological process including bone formation, circadian rhythms, sleep, antioxidant protection, aging, tumor growth, reproduction, and blood pressure regulation.[33] In animals, via receptor-mediated means, melatonin functions in the regulation of sleep, modulation of circadian rhythms, enhancement of immunity, and as a multifunctional oncostatic agent, etc, while retaining its ability to reduce oxidative stress by processes that are, in part, receptor-independent.[4] Suofu et al[34] found that neuronal mitochondria-produced melatonin, binding to MT1 on the mitochondrial membrane (MM), inhibits cytochrome C release, caspase activation, and apoptosis. Mitochondria are also major sites of melatonin production in organisms, and the melatonin synthetic efficiency in mitochondria is much higher than that in cytosol.[35-38] Mitochondria synthesize melatonin de novo and possess an uptake mechanism to maintain high levels of melatonin.[34,35,38,39] Moreover, mitochondria-produced melatonin is not released into the systemic circulation, but rather is primarily used in its cells of origin.[34,35,37] Whether the cells with more mitochondria, such as muscles and hepatocytes, generate more melatonin than other types is currently unknown. The bile of vertebrates contains extremely high levels of melatonin. For example, the level of melatonin in shark bile is several orders of magnitude higher than that in the serum of mammals.[36] These findings suggest that melatonin may be considered as a therapeutic agent at much higher concentrations that are present in the blood.

Both Runx2 and the VDR, as transcription factors, play a key role in osteoblast differentiation, and there is a widely recognized functional relationship between them.[17,18] Melatonin also has a positive effect on the regulation of osteoblasts.[13,26,40-43] However, available information regarding interactive relationships between them is limited. In the present study, we demonstrate that melatonin indirectly regulates Runx2 by direct binding to the VDR, which indicates that the VDR is a novel melatonin-binding receptor.

Melatonin positively regulates Runx2 in many cells and tissues, such as osteogenic[40-44] and chondrogenic[14] differentiation of human MSCs, osteoblastic differentiation of MSCs from rats,[45] co-culture models (transwell or layered) of human MSCs and peripheral blood monocytes,[13] human osteosarcoma-derived Saos2 cells,[46] human periodontal ligament cells and cementoblasts,[47] osteogenic potential of platelet-rich plasma in dental stem-cell cultures,[48] the differentiation of mouse osteoblastic MC3T3-E1 cells,[49] primary bone marrow MSCs from ovariectomized mice,[50] bovine ovarian granulosa cells,[51] a blind mouse model (MMTV-Neu transgenic mice),[52] and pinealectomized[53] or ovariectomized[54] rats. Our study further confirmed that there was no direct interaction between melatonin and Runx2 although melatonin directly penetrates cytomembrane and enters the cell nucleus where it could bind to Runx2. Hence, melatonin may well indirectly regulate Runx2.

The ITC assay documented that there was a direct interaction between melatonin and the VDR and their binding sites were in the C-terminal LBD of the VDR but not in the N-terminal DBD or the hinge region. This indicates that the VDR links with the regulation of melatonin to Runx2 since there is a putative interaction and a functional cooperation between Runx2 and the VDR.[16-25] Moreover, melatonin bound to the C-terminus hormonal receptor binding domain of the VDR, suggesting that there may be a broad-spectrum regulatory mechanism: proteins with a VDR-like hormonal receptor binding domain may have the ability to bind melatonin; this should be further tested by structural analysis in subsequent experiments. Since melatonin and VD3 have similar binding

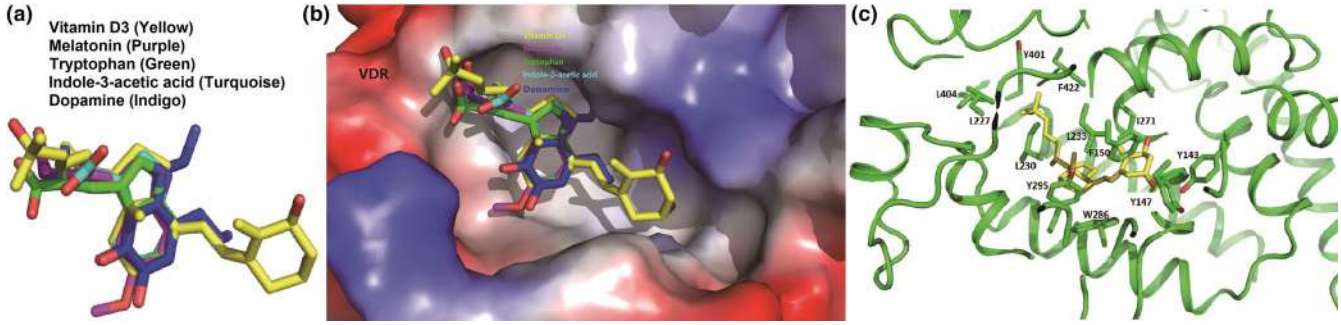

FIGURE 7 Structural comparison and analysis of small molecules. A, Molecular structural comparison among VD3, melatonin, tryptophan, indole-3-acetic acid, and dopamine. B, Structural analysis for small molecules based on the VDR-VD3's crystal structure. C, Structural analysis of the VDR-VD3 complex (PDB: 3CS6)

affinities for the VDR[29] and melatonin is a small indole molecule, we compared chemical structures among VD3, melatonin, and other indole molecules (Trp, IAA, and dopamine). We noticed that there were additional structural similarities among VD3, melatonin, and Trp (Figure 7A). Briefly, they all have a long carbon side chain and at least 2 carbon rings. At the end of the long side chain of VD3 and melatonin molecules is a methyl group, which inserts into the VDR's other hydrophobic cavity (Figure 7B). From the VDR-VD3 crystal structural analysis, the carbon rings locate in the deep hydrophobic cavity of the VDR (Figure 7C).

VD3, formed in the epidermis or provided by the diet, is transported to the liver where it is hydroxylated to form 25-(OH)-vitamin D3 (25(OH)VD3). The 25(OH)VD3 enters the circulation and is then hydroxylated at C1α either in the kidney or peripheral tissues to form $1,25(OH)_2$VD3.[28] In this process, VD3 → 25(OH)VD3 (the major form) → $1,25(OH)_2$VD3 (the strongest activity), they show evident differences in blood concentrations (VD3, 25(OH)VD3 and $1,25(OH)_2$VD3, ~6 nmol/L, ~60 nmol/L; and ~0.02 nmol/L, respectively[55-57]) and in binding affinity for the VDR (VD3, 25(OH)VD3 and $1,25(OH)_2$VD3, Kd ~ 20 μmol/L, ~0.1 μmol/L, and ~0.1 nmol/L, respectively[29,58,59]). The physiological concentration of $1,25(OH)_2$VD3 is distinctly lower than that of melatonin (~0.2 nmol/L[60]) but its affinity to the VDR is far stronger than melatonin (Kd ~ 20 μmol/L, Figure 2). Melatonin and VD3 have similar binding affinities for the VDR,[29] but VD3 can compete with melatonin to bind to the VDR. We found that melatonin and VD3 had similar uptake rates but melatonin's uptake was significantly reduced when VD3 at the same concentrations was simultaneously added. Interestingly, this competitive binding ability was significantly inhibited when the concentration of melatonin was obviously higher than that of VD3, even in the presence of the highest activity $1,25(OH)_2$VD3. These findings suggest that there is a competitive relationship between VD3 and melatonin in binding to the VDR, but this inhibitory effect of VD3 is eliminated by increasing the concentration of melatonin. The reason for this may be that the biological activities of VD3 and its analogues are determined by their ability to induce the VDR transcription rather than the binding affinity for the VDR only.[61]

Our findings documented that melatonin enhanced Runx2 actions by directly binding to the VDR. In contrast, the expression of Runx2 is downregulated by $1,25(OH)_2$VD3 within 24 hours in MC3T3-E1 and ROS 17/2.8, but not in ROS 24.1 cells, which lacks a functional VDR. Furthermore, $1,25(OH)_2$VD3 inhibits Runx2 transcription in ROS 24.1 cells only upon forced expression of the VDR.[62] Studies in primary calvarial cultures reveal that ablation of the VDR enhances osteoblast differentiation.[63] These findings suggest that $1,25(OH)_2$VD3 and melatonin play opposite roles in the regulation of Runx2 by binding to the VDR, which is possibly related to the fact that the biological effects of $1,25(OH)_2$VD3 on osteoblast differentiation and function differ significantly depending upon the maturation state of the cells.[19] Given that Runx2 plays a key role in osteoblast differentiation rather than maturation,[6,8,64,65] these functional differences between $1,25(OH)_2$VD3 and melatonin may be meaningful to coordinate and maintain dynamic equilibrium between differentiation and maturation of osteoblasts.

Other simple indoles such as Trp, IAA, and dopamine did not effectively bind with the VDR although there was an almost negligible interaction between Trp and the VDR. Relative to these small molecules, from melatonin to dopamine, the molecular size gradually decreases. For instance, melatonin contains two carbon rings and two side chains. Trp contains the same two carbon rings but just one side chain. The one side chain is similar to that of melatonin. IAA has a shorter side chain and dopamine contains just one benzene ring. Trp is an essential amino acid that is obtained exclusively from dietary intake in humans. Since Trp is the substrate for the biosynthesis to melatonin and has higher physiological concentrations than melatonin (~30 μmol/L vs. ~0.2 nmol/L[66]) it is very advantageous to melatonin's biosynthesis and physiological functions when the affinity of melatonin to the VDR is far greater than that of Trp. Indeed, this needs to be further examined by structural analysis, etc.

The VDR-Runx2 complex not only contributes to osteogenesis by the action of stabilizing transcriptional complexes at specific promoters[25] but also up-regulates osteocalcin gene expression in osteoblastic cells.[17,18] What's more, the VDR and Runx2 cooperate in the transcriptional regulation of osteopontin.[17,18] Consistent with previous reports,[17,18,24] we further precisely confirmed that the minimum region of combination of Runx2 with the VDR was on the 319-379 position (about 60 amino acid regions) and that the smallest region at where the VDR interacts with Runx2 was at the N-terminus 110-amino acid DBD of the VDR. This suggests that the binding of the VDR with Runx2 is at the DBD but not the LBD of the VDR. Therefore, the DBD of the VDR binds with Runx2 while the LBD of the VDR binds with melatonin. In other words, the VDR directly mediates the interaction between melatonin and Runx2, and the VDR can simultaneously bind with both melatonin and Runx2. Moreover, we further documented that melatonin markedly enhanced the direct interaction between the VDR and Runx2 by both a fluorescence EMSA and co-IP in the MC3T3-E1 cells. This indicates that melatonin indirectly regulates Runx2 by its direct binding with the LBD and the DBD of the VDR, respectively.

The VDR is a DNA-binding transcription factor.[5] To further clarify the effect of Runx2 on the binding of the VDR with its specific DNA sequences, we compared the differences in the VDR specific binding DNA sequences before and after adding Runx2 using EMSA. We found that the DNA-binding ability of the VDR was markedly enhanced after Runx2 was added. These findings to some extent suggest that this interaction facilitates the binding of the VDR with its specific DNA sequences, which is beneficial to osteoblast differentiation due to the rise or drop in transcriptional regulation of target genes associated with osteoblast or osteoclast, respectively.

For the first time, this study provides evidence that the VDR can act as a novel melatonin-binding nuclear receptor and elucidates the connections between the VDR and Runx2 based on a molecular and structural analysis. The discovery that melatonin binds to the C-terminus hormonal receptor binding domain of the VDR may be helpful for further exploring the mechanism of melatonin in terms of how it promotes osteoblast differentiation and for identifying a broad-spectrum regulatory mechanism mentioned above.

ACKNOWLEDGEMENT

This work was financially supported by National Natural Science Foundation of China (81770870).

AUTHOR CONTRIBUTIONS

N. Fang should be considered first author and made substantial contributions to drafting of the manuscript and to acquisition, analysis, and interpretation of data. C. Hu, W. Sun, Y. Xu, Y. Gu, L. Wu, and Q. Peng made substantial contributions to acquisition, analysis, and interpretation of data. RJ Reiter made substantial contributions to critical revision and polish of the manuscript. L. Liu should be considered corresponding author and made substantial contributions to concept/design, drafting, and critical revision of the manuscript and approval of the article.

ORCID

Russel J. Reiter https://orcid.org/0000-0001-6763-4225
Lifeng Liu https://orcid.org/0000-0002-1516-0213

REFERENCES

1. Boga JA, Caballero B, Potes Y, et al. Therapeutic potential of melatonin related to its role as an autophagy regulator: a review. *J Pineal Res*. 2019;66(1):e12534.
2. Majidinia M, Reiter RJ, Shakouri SK, Yousefi B. The role of melatonin, a multitasking molecule, in retarding the processes of ageing. *Ageing Res Rev*. 2018;47:198-213.
3. Tan DX, Reiter RJ. Mitochondria: the birth place, battle ground and the site of melatonin metabolism in cells. *Melatonin Res*. 2019;2(1):44-66.
4. Zhao D, Yu Y, Shen Y, et al. Melatonin synthesis and function: evolutionary history in animals and plants. *Front Endocrinol*. 2019;10:249.
5. Underwood KF, D'Souza DR, Mochin-Peters M, et al. Regulation of RUNX2 transcription factor-DNA interactions and cell proliferation by vitamin D3 (cholecalciferol) prohormone activity. *J Bone Miner Res*. 2012;27(4):913-925.
6. Komori T, Yagi H, Nomura S, et al. Targeted disruption of Cbfa1 results in a complete lack of bone formation owing to maturational arrest of osteoblasts. *Cell*. 1997;89(5):755-764.
7. Bruderer M, Richards RG, Alini M, Stoddart MJ. Role and regulation of RUNX2 in osteogenesis. *Eur Cell Mater*. 2014;28:269-286.
8. Otto F, Thornell AP, Crompton T, et al. Cbfa1, a candidate gene for cleidocranial dysplasia syndrome, is essential for osteoblast differentiation and bone development. *Cell*. 1997;89(5):765-771.
9. Roeder E, Matthews BG, Kalajzic I. Visual reporters for study of the osteoblast lineage. *Bone*. 2016;92:189-195.
10. Zanatta M, Valenti MT, Donatelli L, Zucal C, Dalle Carbonare L. Runx-2 gene expression is associated with age-related changes of bone mineral density in the healthy young-adult population. *J Bone Miner Metab*. 2012;30(6):706-714.
11. Marini F, Cianferotti L, Brandi ML. Epigenetic mechanisms in bone biology and osteoporosis: can they drive therapeutic choices? *Int J Mol Sci*. 2016;17(8):1329.
12. Vimalraj S, Arumugam B, Miranda PJ, Selvamurugan N. Runx2: structure, function, and phosphorylation in osteoblast differentiation. *Int J Biol Macromol*. 2015;78:202-208.
13. Maria S, Samsonraj RM, Munmun F, et al. Biological effects of melatonin on osteoblast/osteoclast cocultures, bone, and quality of life: implications of a role for MT2 melatonin receptors, MEK1/2, and MEK5 in melatonin-mediated osteoblastogenesis. *J Pineal Res*. 2018;64(3):e12465.

14. Gao W, Lin M, Liang A, et al. Melatonin enhances chondrogenic differentiation of human mesenchymal stem cells. *J Pineal Res*. 2014;56(1):62-70.
15. Katayama Y. Vitamin D receptor: a critical regulator of inter-organ communication between skeletal and hematopoietic systems. *J Steroid Biochem Mol Biol*. 2019;190:281-283.
16. Stephens AS, Morrison NA. Novel target genes of RUNX2 transcription factor and 1,25-dihydroxy vitamin D3. *J Cell Biochem*. 2014;115(9):1594-1608.
17. Paredes R, Arriagada G, Cruzat F, et al. Bone-specific transcription factor Runx2 interacts with the 1alpha,25-dihydroxy vitamin D3 receptor to up-regulate rat osteocalcin gene expression in osteoblastic cells. *Mol Cell Biol*. 2004;24(20):8847-8861.
18. Paredes R, Arriagada G, Cruzat F, et al. The Runx2 transcription factor plays a key role in the 1alpha,25-dihydroxy vitamin D3-dependent upregulation of the rat osteocalcin (OC) gene expression in osteoblastic cells. *J Steroid Biochem Mol Biol*. 2004;89–90(1–5):269-271.
19. Meyer MB, Benkusky NA, Lee CH, Pike JW. Genomic determinants of gene regulation by 1,25-dihydroxy vitamin D3 during osteoblast-lineage cell differentiation. *J Biol Chem*. 2014;289(28):19539-19554.
20. Shen Q, Christakos S. The vitamin D receptor, Runx2, and the Notch signaling pathway cooperate in the transcriptional regulation of osteopontin. *J Biol Chem*. 2005;280(49):40589-40598.
21. Sowa AK, Kaiser FJ, Eckhold J, et al. Functional interaction of osteogenic transcription factors Runx2 and Vdr in transcriptional regulation of Opn during soft tissue calcification. *Am J Pathol*. 2013;183(1):60-68.
22. Han MS, Che X, Cho GH, et al. Functional cooperation between vitamin D receptor and Runx2 in vitamin D-induced vascular calcification. *PLoS ONE*. 2013;8(12):e83584.
23. Jia Z, Wang S, He D, et al. Role of calcium in the regulation of bone morphogenetic protein 2, runt-related transcription factor 2 and Osterix in primary renal tubular epithelial cells by the vitamin D receptor. *Mol Med Rep*. 2015;12(2):2082-2088.
24. Bruna C, Arriagada G, Lian JB, et al. Crystallization and preliminary X-ray analysis of a domain in the Runx2 transcription factor that interacts with the 1alpha,25 dihydroxy vitamin D3 receptor. *J Cell Biochem*. 2007;101(3):785-789.
25. Marcellini S, Bruna C, Henríquez JP, et al. Evolution of the interaction between Runx2 and VDR, two transcription factors involved in osteoblastogenesis. *BMC Evol Biol*. 2010;10:78.
26. Prado NJ, Casarotto M, Calvo JP, et al. Antiarrhythmic effect linked to melatonin cardiorenal protection involves AT1 reduction and Hsp70-VDR increase. *J Pineal Res*. 2018;65(4):e12513.
27. Rose AB, Broach JR. Propagation and expression of cloned genes in yeast: 2-microns circle-based vectors. *Methods Enzymol*. 1990;185:234-279.
28. Tuckey RC, Cheng CYS, Slominski AT. The serum vitamin D metabolome: what we know and what is still to discover. *J Steroid Biochem Mol Biol*. 2019;186:4-21.
29. Chen TC, Persons KS, Lu Z, Mathieu JS, Holick MF. An evaluation of the biologic activity and vitamin D receptor binding affinity of the photoisomers of vitamin D3 and previtamin D3. *J Nutr Biochem*. 2000;11(5):267-272.
30. Evans RM. The steroid and thyroid hormone receptor superfamily. *Science*. 1988;240(4854):889-895.
31. Mutchie TR, Yu OB, Di Milo ES, Arnold LA. Alternative binding sites at the vitamin D receptor and their ligands. *Mol Cell Endocrinol*. 2019;485:1-8.
32. Shaffer PL, Gewirth DT. Structural basis of VDR-DNA interactions on direct repeat response elements. *EMBO J*. 2002;21(9):2242-2252.
33. Liu L, Xu Y, Reiter RJ, et al. Inhibition of ERK1/2 signaling pathway is involved in melatonin's antiproliferative effect on human MG-63 osteosarcoma cells. *Cell Physiol Biochem*. 2016;39(6):2297-2307.
34. Suofu Y, Li W, Jean-Alphonse FG, et al. Dual role of mitochondria in producing melatonin and driving GPCR signaling to block cytochrome c release. *Proc Natl Acad Sci U S A*. 2017;114(38):e7997-e8006.
35. He C, Wang J, Zhang Z, et al. Mitochondria synthesize melatonin to ameliorate its function and improve mice oocyte's quality under in vitro conditions. *Int J Mol Sci*. 2016;17(6):E939.
36. Tan D, Manchester LC, Reiter RJ, Qi W, Hanes MA, Farley NJ. High physiological levels of melatonin in the bile of mammals. *Life Sci*. 1999;65(23):2523-2529.
37. Venegas C, García JA, Escames G, et al. Extrapineal melatonin: analysis of its subcellular distribution and daily fluctuations. *J Pineal Res*. 2012;52(2):217-227.
38. Wang L, Feng C, Zheng X, et al. Plant mitochondria synthesize melatonin and enhance the tolerance of plants to drought stress. *J Pineal Res*. 2017;63(3):e12429.
39. Huo X, Wang C, Yu Z, et al. Human transporters, PEPT1/2, facilitate melatonin transportation into mitochondria of cancer cells: an implication of the therapeutic potential. *J Pineal Res*. 2017;62(4):e12390.
40. Lee S, Le NH, Kang D. Melatonin alleviates oxidative stress-inhibited osteogenesis of human bone marrow-derived mesenchymal stem cells through AMPK activation. *Int J Med Sci*. 2018;15(10):1083-1091.
41. Maria S, Swanson MH, Enderby LT, et al. Melatonin-micronutrients osteopenia treatment study (MOTS): a translational study assessing melatonin, strontium (citrate), vitamin D3 and vitamin K2 (MK7) on bone density, bone marker turnover and health related quality of life in postmenopausal osteopenic women following a one-year double-blind RCT and on osteoblast-osteoclast co-cultures. *Aging*. 2017;9(1):256-285.
42. Zhang L, Su P, Xu C, et al. Melatonin inhibits adipogenesis and enhances osteogenesis of human mesenchymal stem cells by suppressing PPARγ expression and enhancing Runx2 expression. *J Pineal Res*. 2010;49(4):364-372.
43. Zhang L, Zhang J, Ling Y, et al. Sustained release of melatonin from poly (lactic-co-glycolic acid) (PLGA) microspheres to induce osteogenesis of human mesenchymal stem cells in vitro. *J Pineal Res*. 2013;54(1):24-32.
44. Lai M, Jin Z, Tang Q, Lu M. Sustained release of melatonin from TiO2 nanotubes for modulating osteogenic differentiation of mesenchymal stem cells in vitro. *J Biomater Sci Polym Ed*. 2017;28(15):1651-1664.
45. Dong P, Gu X, Zhu G, Li M, Ma B, Zi Y. Melatonin induces osteoblastic differentiation of mesenchymal stem cells and promotes fracture healing in a rat model of femoral fracture via neuropeptide Y/neuropeptide Y receptor Y1 signaling. *Pharmacology*. 2018;102(5–6):272-280.
46. Matsumura H, Ogata Y. Melatonin regulates human bone sialoprotein gene transcription. *J Oral Sci*. 2014;56(1):67-76.

47. Bae WJ, Park JS, Kang SK, Kwon IK, Kim EC. Effects of melatonin and its underlying mechanism on ethanol-stimulated senescence and osteoclastic differentiation in human periodontal ligament cells and cementoblasts. *Int J Mol Sci*. 2018;19(6):1742.
48. Otero L, Carrillo N, Calvo-Guirado JL, Villamil J, Delgado-Ruíz RA. Osteogenic potential of platelet-rich plasma in dental stem-cell cultures. *Br J Oral Maxillofac Surg*. 2017;55(7):697-702.
49. Park KH, Kang JW, Lee EM, et al. Melatonin promotes osteoblastic differentiation through the BMP/ERK/Wnt signaling pathways. *J Pineal Res*. 2011;51(2):187-194.
50. Xu L, Zhang L, Wang Z, et al. Melatonin suppresses estrogen deficiency-induced osteoporosis and promotes osteoblastogenesis by inactivating the NLRP3 inflammasome. *Calcif Tissue Int*. 2018;103(4):400-410.
51. Wang S, Liu W, Pang X, Dai S, Liu G. The mechanism of melatonin and its receptor MT2 involved in the development of bovine granulosa cells. *Int J Mol Sci*. 2018;19(7):2028.
52. Witt-Enderby PA, Slater JP, Johnson NA, et al. Effects on bone by the light/dark cycle and chronic treatment with melatonin and/or hormone replacement therapy in intact female mice. *J Pineal Res*. 2012;53(4):374-384.
53. Palin LP, Polo TOB, Batista FRS, et al. Daily melatonin administration improves osseointegration in pinealectomized rats. *J Appl Oral Sci*. 2018;26:e20170470.
54. Gürler EB, Çilingir-Kaya ÖT, Peker Eyüboglu I, et al. Melatonin supports alendronate in preserving bone matrix and prevents gastric inflammation in ovariectomized rats. *Cell Biochem Funct*. 2019;37(2):102-112.
55. Shah I, Petroczi A, Naughton DP. Exploring the role of vitamin D in type 1 diabetes, rheumatoid arthritis, and Alzheimer disease: new insights from accurate analysis of 10 forms. *J Clin Endocrinol Metab*. 2014;99(3):808-816.
56. Slominski AT, Kim TK, Li W, et al. Detection of novel CYP11A1-derived secosteroids in the human epidermis and serum and pig adrenal gland. *Sci Rep*. 2015;5:14875.
57. Tang JCY, Nicholls H, Piec I, et al. Reference intervals for serum 24,25-dihydroxyvitamin D and the ratio with 25-hydroxyvitamin D established using a newly developed LC-MS/MS method. *J Nutr Biochem*. 2017;46:21-29.
58. Mottershead DG, Polly P, Lyons RJ, Sutherland RL, Watts CK. High activity, soluble, bacterially expressed human vitamin D receptor and its ligand binding domain. *J Cell Biochem*. 1996;61(3):325-337.
59. Vertino AM, Bula CM, Chen JR, et al. Nongenotropic, anti-apoptotic signaling of 1alpha,25(OH)2-vitamin D3 and analogs through the ligand binding domain of the vitamin D receptor in osteoblasts and osteocytes. Mediation by Src, phosphatidylinositol 3-, and JNK kinases. *J Biol Chem*. 2005;280(14):14130-14137.
60. Sae-Teaw M, Johns J, Johns NP, Subongkot S. Serum melatonin levels and antioxidant capacities after consumption of pineapple, orange, or banana by healthy male volunteers. *J Pineal Res*. 2013;55(1):58-64.
61. Hansen CM, Mathiasen IS, Binderup L. The anti-proliferative and differentiation-inducing effects of vitamin D analogs are not determined by the binding affinity for the vitamin D receptor alone. *J Investig Dermatol Symp Proc*. 1996;1(1):44-48.
62. Drissi H, Pouliot A, Koolloos C, et al. 1,25-$(OH)_2$-vitamin D3 suppresses the bone-related Runx2/Cbfa1 gene promoter. *Exp Cell Res*. 2002;274(2):323-333.
63. Sooy K, Sabbagh Y, Demay MB. Osteoblasts lacking the vitamin D receptor display enhanced osteogenic potential in vitro. *J Cell Biochem*. 2005;94(1):81-87.
64. Ducy P, Zhang R, Geoffroy V, Ridall AL, Karsenty G. Osf2/Cbfa1: a transcriptional activator of osteoblast differentiation. *Cell*. 1997;89(5):747-754.
65. Nakashima K, Zhou X, Kunkel G, et al. The novel zinc finger-containing transcription factor osterix is required for osteoblast differentiation and bone formation. *Cell*. 2002;108(1):17-29.
66. Sagara Y, Okatani Y, Yamanaka S, Kiriyama T. Determination of plasma 5-hydroxytryptophan, 5-hydroxytryptamine, 5-hydroxyindoleacetic acid, tryptophan and melatonin by high-performance liquid chromatography with electrochemical detection. *J Chromatogr*. 1988;431(1):170-176.

How to cite this article: Fang N, Hu C, Sun W, et al. Identification of a novel melatonin-binding nuclear receptor: Vitamin D receptor. *J Pineal Res*. 2020;68:e12618. https://doi.org/10.1111/jpi.12618